PNAS RESEARCH ARTICLE | MICROBIOLOGY

Autophagic membranes participate in hepatitis B virus nucleocapsid assembly, precore and core protein trafficking, and viral release

Ja Yeon Kim Chu[a,1], Yu-Chen Chuang[a,1], Kuen-Nan Tsai[a], Jessica Pantuso[a], Yuji Ishida[b,c], Takeshi Saito[a,b], and Jing-hsiung James Ou[a,2]

Edited by Peter Sarnow, Stanford University School of Medicine, Stanford, CA; received February 2, 2022; accepted June 5, 2022

Hepatitis B virus (HBV) DNA replication takes place inside the viral core particle and is dependent on autophagy. Here we show that HBV core particles are associated with autophagosomes and phagophores in cells that productively replicate HBV. These autophagic membrane-associated core particles contain almost entirely the hypophosphorylated core protein and are DNA replication competent. As the hyperphosphorylated core protein can be localized to phagophores and the dephosphorylation of the core protein is associated with the packaging of viral pregenomic RNA (pgRNA), these results are in support of the model that phagophores can serve as the sites for the packaging of pgRNA. In contrast, in cells that replicate HBV, the precore protein derivatives, which are related to the core protein, are associated with autophagosomes but not with phagophores via a pathway that is independent of its signal peptide. Interestingly, when the core protein is expressed by itself, it is associated with phagophores but not with autophagosomes. These observations indicate that autophagic membranes are differentially involved in the trafficking of precore and core proteins. HBV induces the fusion of autophagosomes and multivesicular bodies and the silencing of Rab11, a regulator of this fusion, is associated with the reduction of release of mature HBV particles. Our studies thus indicate that autophagic membranes participate in the assembly of HBV nucleocapsids, the trafficking of HBV precore and core proteins, and likely also the egress of HBV particles.

hepatitis B virus | autophagy | phagophores | autophagosomes | HBV protein trafficking

Significance

Hepatitis B virus (HBV) is an important human pathogen that can cause severe liver diseases. It can induce autophagy, a cellular pathway that is important for maintaining cellular homeostasis, to support its replication. In this report, we demonstrate that autophagic membranes participate in HBV DNA replication, mediate the trafficking of HBV proteins, and likely also regulate the release of mature HBV particles. Our study provides detailed information for understanding the roles of phagophores, autophagosomes, and amphisomes in the lifecycle of HBV and opens a new avenue for the development of novel anti-HBV drugs.

Hepatitis B virus (HBV) chronically infects nearly 300 million people worldwide and can cause severe liver diseases, including cirrhosis and hepatocellular carcinoma (1, 2). HBV is an enveloped virus with a small 3.2-kb circular and partially double-stranded DNA (dsDNA) genome (3). The HBV genome contains four overlapping genes termed *S*, *C*, *P*, and *X* genes. The *S* gene contains three in-phase translation initiation codons and expresses three cocarboxy-terminal envelope proteins collectively known as the surface antigen (HBsAg). The *C* gene also contains two in-phase ATG codons. The translation initiating from the downstream ATG codon generates the 21-kDa core protein, which forms the viral core particle that displays the core antigenic determinant (HBcAg). The translation initiating from the upstream ATG codon produces a 25-kDa protein termed the precore protein, which contains the entire sequence of the core protein plus an amino-terminal extension of 29 amino acids (i.e., the precore sequence). The N terminus of the precore sequence contains a signal peptide. This signal peptide directs the precore protein to the endoplasmic reticulum (ER) and is cotranslationally removed by the signal peptidase located in the lumen of ER to generate the precore protein derivative termed p22 (4). p22 is either translocated into the ER and further cleaved at multiple sites at its C-terminal arginine-rich domain by a furin-like protease in the *trans*-Golgi network and secreted as a dimer (5–7) or released back into the cytosol (8). The secreted precore derivatives are known as the e antigen (HBeAg). HBeAg is detected in the serum of HBV patients and immunologically distinct from HBcAg. The arginine-rich domain shared by p22 and the core protein contains a nuclear localization signal (8), which promotes the nuclear localization of p22 and the core protein (9). The *P* gene codes for the viral DNA polymerase, which is also a reverse transcriptase, and the *X* gene codes for a regulatory protein.

The replication of HBV DNA takes place inside the core particle. The HBV core protein packages the pregenomic RNA (pgRNA), which is also the mRNA of the core protein and the polymerase, to form the core particle. The pgRNA is then converted to the circular and partially dsDNA genome by the viral DNA polymerase that is also packaged (10–12). The phosphorylation of the core protein is required for the packaging of the pgRNA and its dephosphorylation occurs during the packaging of the

Author affiliations: [a]Department of Molecular Microbiology and Immunology, University of Southern California Keck School of Medicine, Los Angeles, CA 90033; [b]Department of Medicine, Division of Gastrointestinal and Liver Diseases, University of Southern California Keck School of Medicine, Los Angeles, CA 90033; and [c]Research and Development Department, PhoenixBio, Co., Ltd, Kagamiyama, Higashi-Hiroshima City, 739-0046 Japan

Author contributions: J.Y.K.C., Y.-C.C., and J.-h.J.O. designed research; J.Y.K.C., Y.-C.C., K.-N.T., and J.P. performed research; Y.I. and T.S. contributed new reagents/analytic tools; J.Y.K.C., Y.-C.C., and J.-h.J.O. analyzed data; and J.Y.K.C., Y.-C.C., and J.-h.J.O. wrote the paper.

The authors declare no competing interest.

This article is a PNAS Direct Submission.

[1]J.Y.K.C. and Y.-C.C. contributed equally to this work.

[2]To whom correspondence may be addressed. Email: jamesou@usc.edu.

This article contains supporting information online at http://www.pnas.org/lookup/suppl/doi:10.1073/pnas.2201927119/-/DCSupplemental.

Published July 18, 2022.

pgRNA and is required for HBV DNA replication (13, 14). The core particle then interacts with viral envelope proteins in intracellular membranes to form the mature virion (10, 15), which is released from cells via a process that involves the multivesicular bodies (MVBs) and the endosomal sorting complex required for transport (ESCRT) machinery (16–18).

Autophagy is a catabolic process that is important for maintaining cellular homeostasis. In the early stage of autophagy, membrane crescents, known as phagophores or isolation membranes, are formed in the cytosol. The membranes of phagophores subsequently expand to form an enclosed double-membrane structure known as the autophagosome. Autophagosomes mature by fusing with lysosomes to form autolysosomes, in which the cargoes of autophagosomes are digested by lysosomal enzymes for recycling (19). In addition to fusing with lysosomes, autophagosomes may also fuse with MVBs to form amphisomes. Amphisomes may fuse with lysosomes or, alternatively, fuse with plasma membranes for the release of its cargos in a process known as secretory autophagy (20–22). The regulation of autophagy involves more than 30 autophagy-related genes (ATG) (23). For example, ATG5 and ATG12, which are covalently linked, complex with ATG16L to form phagophores. The microtubule-associated protein light-chain 3 (LC3), a cytosolic protein, becomes lipidated during autophagy and replaces the ATG5-ATG12-ATG16L complex on expanding phagophores to complete the formation of autophagosome (24, 25). ATG5, ATG12, or ATG16L is hence often used as the marker for phagophores, and lipidated LC3 is used as the marker for autophagosomes (26).

Many viruses, including HBV, can perturb the autophagic pathway to promote their own replications (27). HBV can activate the early autophagic pathway to enhance its DNA replication (28). In addition, studies from transgenic mice carrying an overlength HBV DNA genome with liver-specific knockout of ATG5 confirmed an essential role of autophagy in HBV DNA replication in vivo (29). Although it has been very well documented that HBV could induce autophagy to promote its own replication, the detailed molecular mechanism by which autophagy and autophagic membranes regulate HBV replication remains largely unclear.

In this report, we examined the relationship between autophagic membranes and HBV core particles to understand how autophagy might regulate HBV DNA replication. We found that HBV core particles that contained replicating HBV DNA were associated with autophagosomes and phagophores, and phagophores could apparently serve as the sites for the packaging of HBV pgRNA. We also found that the precore protein was associated with autophagosomes via a pathway independent of its signal peptide. Interestingly, when the core protein was expressed by itself, it was associated with phagophores but not with autophagosomes. These results indicate distinct relationships between autophagic membranes and intracellular trafficking of core and precore proteins. Our further studies indicate that HBV induced the fusion between autophagosomes and MVBs, and the silencing of Rab11, a small GTPase involved in this fusion, was associated with the reduction of release of mature HBV particles from cells. Together, these results indicate that autophagic membranes participate in the assembly of HBV nucleocapsids, the trafficking of precore and core proteins, and likely also the egress of HBV.

Results

HBV Core Particles Colocalize with Autophagosomes in HBV-Infected Hepatocytes. Previous studies indicated that HBV could induce autophagy in liver-derived cell lines, including Huh7 and HepG2 cells. However, whether HBV can induce autophagy in primary human hepatocytes after infection had not been demonstrated. To test this possibility, we infected PXB cells, which were human hepatocytes isolated from humanized uPA/SCID mice (30), with HBV. At day 5 postinfection, cells were lysed for immunoblot analysis. As shown in Fig. 1*A*, HBV induced the lipidation of LC3, which is a marker of autophagy, without affecting the level of p62, a protein degraded by autophagy. This result is consistent with the previous reports, which indicated that HBV could induce autophagosomes without inducing autophagic protein degradation (29). The analysis using an antibody that recognized both the precore protein and the denatured core protein (i.e., the antibody directed against HBeAg, see below) revealed multiple precore/core protein bands in HBV-infected cells but not in mock-infected cells. To confirm the induction of the autophagic response by HBV, we also performed immunofluorescence microscopy. As shown in Fig. 1*B*, although few LC3 puncta (i.e., autophagosomes) were detected in mock-infected cells, a significant amount of LC3 puncta was detected in HBV-infected cells, confirming the induction of autophagosomes by HBV. We also analyzed HBV core particles using an antibody that specifically recognized HBcAg and not HBeAg (see below). Interestingly, HBcAg colocalized extensively with LC3 puncta, indicating the possible association of HBV core particles with autophagosomes. Due to the difficulty to obtain human hepatocytes on a frequent basis, our subsequent studies were conducted using Huh7 hepatoma cells that had been transfected with the 1.3mer overlength HBV genomic DNA.

HBV Core Particles Are Associated with Purified Autophagosomes. To confirm the association of HBV core particles with autophagosomes, we used a two-step purification procedure that we recently developed to purify autophagosomes. This two-step purification procedure involves first, the isolation of cellular membranes, and second, the affinity purification of autophagosomes from isolated membranes. We had previously established a Huh7 hepatoma cell line that stably expressed the green fluorescent protein (GFP)-LC3 fusion protein (Huh7-GFP-LC3) (31). To purify HBV-induced autophagosomes, Huh7-GFP-LC3 cells were transfected with the control vector pUC19 or the 1.3mer overlength HBV genome. Huh7 cells that did not express the GFP-LC3 fusion protein were also transfected with the 1.3mer HBV genome to serve as the control. Cellular membranes were isolated by membrane flotation in a discontinuous sucrose gradient after ultracentrifugation. As shown in Fig. 2*A*, LC3-II and GFP LC3-II, which are markers of autophagosomes, were efficiently separated from their nonlipidated cytosolic forms, LC3-I and GFP–LC3-I. GAPDH, a cytosolic protein, was detected in the

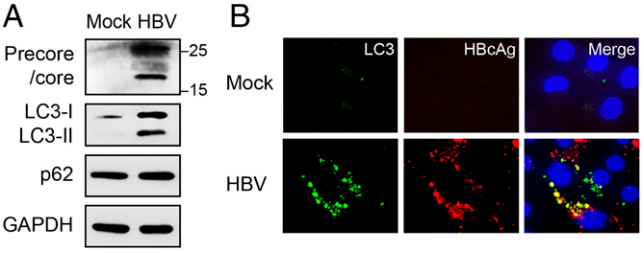

Fig. 1. Colocalization of HBV-induced autophagosomes with HBcAg in human hepatocytes by HBV infection. PXB cells were infected with HBV (MOI = 100) for 5 d. Cells were lysed for Western blot analysis (*A*) or fixed and stained for LC3 (green) and HBcAg (red) (*B*). In *A*, LC3-I and LC3-II are the nonlipidated and lipidated forms of LC3, respectively, and in *B*, DAPI was used to stain nuclei. The cells were examined at 40x magnification.

cytosolic fractions (fractions 5 to 10) as expected. Immunoblot analysis using the anti-HBeAg antibody that did not distinguish between denatured precore and core proteins revealed a precore/core protein band in both the membrane fraction (fraction 3) and the cytosolic fractions (7–10) for cells transfected with the HBV genomic DNA.

We had also analyzed replicating HBV DNA in the sucrose gradient by Southern blot. Interestingly, a strong HBV DNA signal was detected in the membrane fraction (Fig. 2*B*). The analysis of the pgRNA packaged in core particles also revealed that a significant fraction of pgRNA was associated with the membrane fraction (Fig. 2*C*). These results indicate the possible association of HBV pgRNA packaging and DNA replication with membranes.

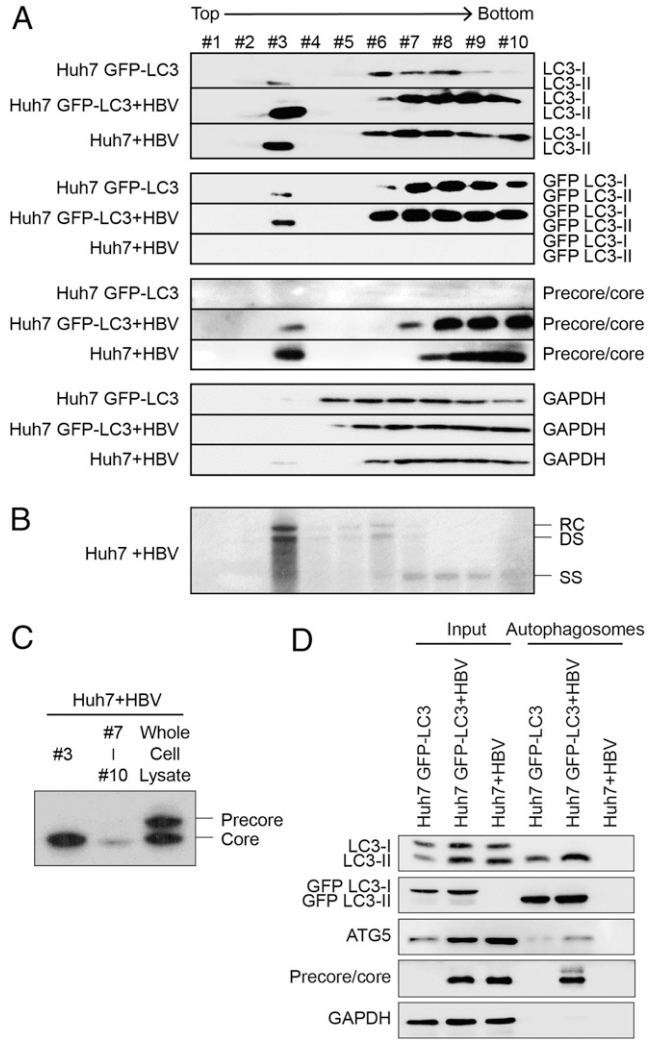

Fig. 2. Purification of autophagosomes from cells transfected with the HBV genomic DNA. (*A*) Stable Huh7-GFP-LC3 cells transfected with pUC19 or the 1.3mer HBV genome, and Huh7 cells transfected with the 1.3mer HBV genome were lysed 48 h later with a hypotonic buffer and fractionated in a discontinuous sucrose gradient. Individual fractions were analyzed by immunoblotting. The top and the bottom of the gradient are indicated. (*B*) Southern-blot analysis of core particle-associated HBV DNA in individual sucrose fractions of Huh7+HBV cells. DS, double-stranded linear DNA; RC, relaxed circular DNA; and SS, single-stranded DNA. (*C*) Primer-extension analysis of pgRNA packaged in core particles in fraction 3 or pooled fractions 7 to 10 of Huh7+HBV cells. Total cellular RNA was used as the control in the analysis. (*D*) Fraction 3 shown in *A* was isolated, and autophagosomes in this fraction were affinity-purified using anti-GFP beads and analyzed by immunoblot. Total cell lysates were also analyzed to serve as the input control.

Autophagosomes in fraction 3 were subsequently affinity-purified using the anti-GFP antibody. The purified autophagosomes as well as total cell lysates (i.e., the input control) were then subjected to immunoblot analysis. As shown in Fig. 2*D*, in agreement with the previous reports (28, 32) and the results shown in Fig. 1*A*, HBV increased the level of LC3-II. A slight increase of the GFP–LC3-II band was also detected. In contrast to HBV-infected PXB cells, which generated multiple precore and core protein bands, Huh7 cells transfected by the HBV genomic DNA produced predominantly the 21-kDa core protein (also see below). When autophagosomes purified from GFP–LC3-II cells transfected with the HBV DNA (Huh7-GFP-LC3+HBV) were analyzed by immunoblot, LC3-II, GFP–LC3-II, ATG5, and the 21-kDa core protein were detected. The detection of a low level of ATG5 with autophagosomes was not surprising, as some of the purified autophagosomes were likely membranes transitioning from phagophores to autophagosomes and therefore positive for both ATG5 and LC3-II. An additional protein band, which migrated slightly more slowly than the core protein band, was also detected. This protein band was presumably the precore protein derivative p22 (also see below). The association of the core protein with purified autophagosomes was consistent with the results shown in Fig. 1*B*, which indicated the colocalization of the core particles with autophagosomes. This association of p22 and the core protein with autophagosomes was not due to contamination, as it was not detected in Huh7 cells transfected with the 1.3mer HBV genome (Huh7+HBV), which served as the negative control.

Association of HBV Core Particles with Autophagosomes Is Independent of Precore Protein, HBsAg, and DNA Replication. To test whether the association of the core protein with autophagosomes was mediated by the precore protein, which contained a signal peptide for membrane-targeting, Huh7-GFP-LC3 cells were transfected with the 1.3mer HBV genome that was incapable of expressing only the precore protein. This precore mutant contains a G-to-A mutation at nucleotide 1896, which converted a TGG codon to a TGA termination codon and abolished the expression of the precore protein without affecting the expression of the core protein or other HBV genes (33). Autophagosomes were then purified from cells for immunoblot analysis. As shown in Fig. 3*A*, the precore mutation did not affect the association of the 21-kDa protein with autophagosomes, although it led to the loss of two protein bands with slightly faster and slower mobilities on the gel than the 21-kDa protein band. These results confirmed that the 21-kDa protein was indeed the core protein and the slower migrating protein band was the precore protein-derivative p22. The faster migrating band was presumably a p22-derivative likely generated by cleavage at the C-terminal arginine-rich domain. These results also demonstrated that the association of the core protein with autophagosomes was precore-independent.

To confirm that the association of the HBV core particles with autophagosomes was indeed independent of the precore protein, we conducted the immunofluorescence staining experiments using antibodies directed against HBcAg (i.e., the core particle) or HBeAg. As shown in Fig. 3*B* and *C*, HBV core particles were detected in both the cytoplasm and the nucleus and there was a high degree of colocalization of cytoplasmic core with autophagosomes, irrespective of whether the cells were transfected with the WT genome or the precore-negative mutant (PC MT) genome (Fig. 3*D*). In contrast, HBeAg was detected mostly in the cytoplasm and partially colocalized with autophagosomes in cells transfected with the WT HBV genome (Fig. 3*B* and *D*). It was not

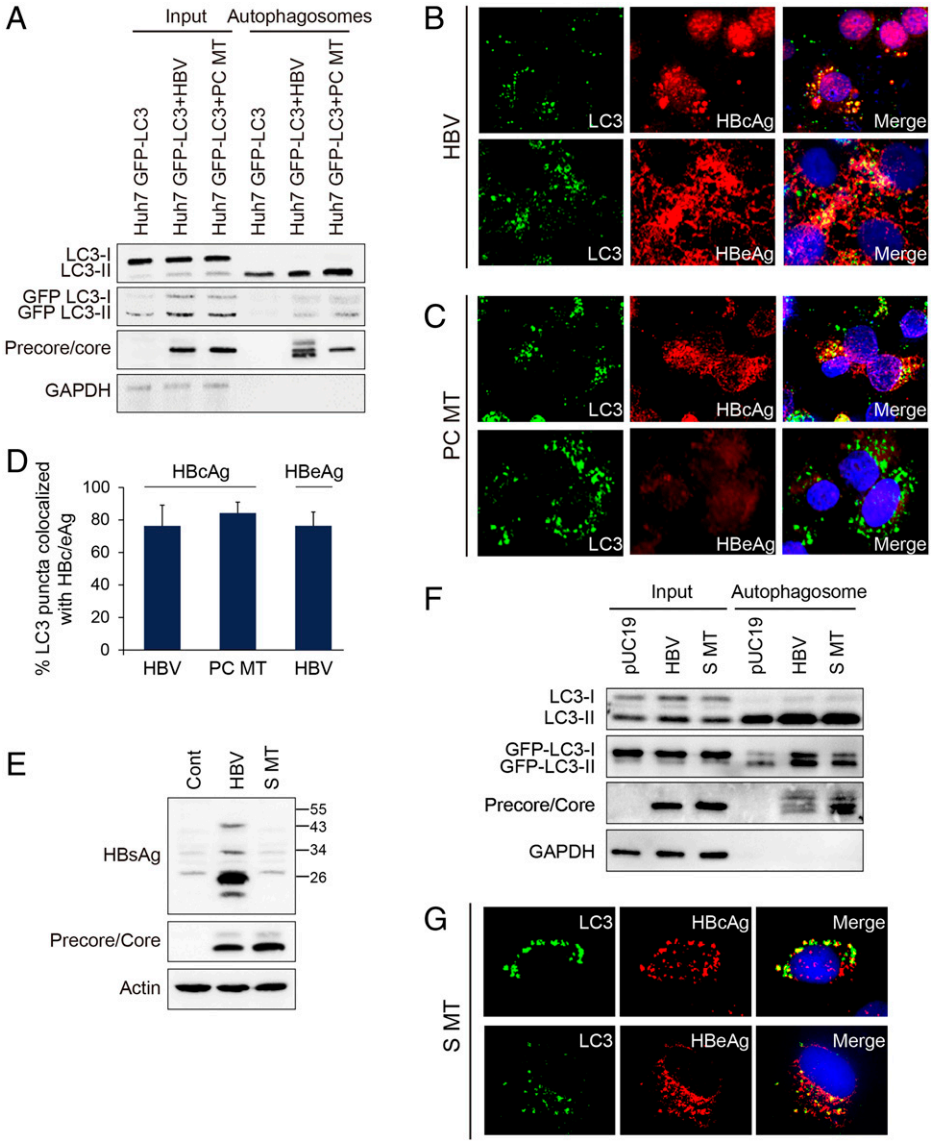

Fig. 3. Association of HBV core particles with autophagosomes in cells transfected with the HBV genomic DNA. Huh7-GFP-LC3 cells were transfected with pUC19, p1.3xHBV, p1.3xHBV PC MT, or p1.3xHBV S MT for 48 h. (*A*) Autophagosomes purified by the two-step protocol were subjected to immunoblot analysis. Total cell lysates were used as the input control. (*B*) Huh7-GFP-LC3 cells transfected with p1.3xHBV were immunofluorescence-stained for HBcAg and HBeAg (red) using their respective antibodies for their colocalization with GFP-LC3 puncta. DAPI was used to stain nuclei (blue). (*C*) The study was conducted the same way as in *B*, with the exception that cells were transfected with p1.3xHBV PC MT. (D) Percentages of GFP-LC3 puncta that were positive for HBcAg and HBeAg in HBV WT cells or PC MT cells. The results represent the average of >50 cells. (E) Immunoblot analysis of cells transfected with pUC19, p1.3xHBV or the p1.3xHBV S-negative mutant (S MT). The numbers (in kDa) denote the locations of molecular weight markers. (F) Immunoblot analysis of total cell lysates (input) and autophagosomes purified from cells transfected with pUC19, p1.3xHBV or S MT. (G) Colocalization analysis of HBcAg or HBeAg (red) with autophagosomes (green). The cells were examined at 40x magnification.

detected in cells transfected with the PC MT DNA (Fig. 3*C*). These results confirmed that the association of the HBV core particles with autophagosomes was independent of the precore protein and demonstrated that precore protein derivatives were also associated with autophagosomes.

We also investigated whether the association of core particles with autophagosomes was mediated by surface proteins by introducing a T-to-A mutation at nucleotide 223, which converted codon 22 of the small S protein sequence to a premature termination codon, to prevent the proper expression of all three surface proteins. The HBV genome with this S gene mutation (S MT) was then transfected into Huh7-GFP-LC3 cells. As shown in Fig. 3*E*, the S gene mutation led to the loss of all three surface proteins without affecting the expression of precore and core proteins. It also abolished the secretion of HBsAg into the incubation media without affecting the secretion of HBeAg (*SI Appendix*, Fig. S1 *A* and *B*). We next conducted the immunoblot analysis on purified autophagosomes. As shown in Fig. 3*F*, the association of the core protein and the precore protein derivatives with autophagosomes was not affected by the loss of surface proteins. The immunofluorescence staining of HBcAg and HBeAg also confirmed their association with autophagic puncta in cells (Fig. 3*G*). The HBV DNA replication also did not appear to be essential for precore and core proteins to become associated with autophagosomes, as the treatment of cells with entecavir, a deoxyguanosine analog that inhibited the HBV DNA polymerase activity (34) and abolished HBV DNA replication (*SI Appendix*, Fig. S1*C*), had no effect on the association of these two proteins with autophagosomes (*SI Appendix*, Fig. S1*D*).

Precore and Core Proteins Are Peripherally Associated with Autophagosomes. To further study the topological relationship between core particles and autophagosomes, we conducted the

trypsin digestion experiment. Proteins that are peripherally associated with autophagosomes would be sensitive to trypsin digestion, and those that are located in the lumen of autophagosomes would be resistant. Autophagosomes were purified from Huh7-GFP-LC3+HBV cells and then treated with trypsin. As shown in Fig. 4*A*, the core protein was completely digested by trypsin regardless of whether it was expressed by the WT HBV genome or the PC MT mutant, indicating that it was only peripherally associated with autophagosomes. Interestingly, precore protein derivatives expressed by the WT HBV genome were also sensitive to trypsin, indicating that they were also located on the outside of autophagosomal membranes. To confirm this result, we expressed the precore protein by itself in Huh7-GFP-LC3 cells followed by the purification of autophagosomes for trypsin digestion. As shown in the same figure, the precore protein derivatives associated with autophagosomes were sensitive to trypsin digestion, confirming that they were indeed peripherally associated with autophagosomes. As a control, we also analyzed LC3-II, which is associated with both inner and outer membranes of autophagosomes. As shown in the same figure, LC3-II was partially resistant to trypsin digestion. However, this partial resistance was lost if membranes were solubilized with 0.1% Nonidet P-40 (Nonidet P-40), a nonionic detergent. In contrast, apolipoprotein E (ApoE), which resides in the lumen of autophagosomes (35), was not sensitive to trypsin digestion unless the membranes were solubilized by Nonidet P-40. These results indicated that HBV precore protein derivatives and core particles were only peripherally associated with autophagosomes.

The peripheral association of the precore protein derivatives with autophagosomes was interesting and raised the possibility that these protein species might be derived from p22 that was released back into the cytosol after the removal of its signal peptide. To investigate this possibility, we expressed the precore protein, its derivative p22 without its signal peptide, and the core protein separately in Huh7-GFP-LC3 cells and used the two-step purification procedure to purify autophagosomes for immunoblot analysis. As shown in Fig. 4*B*, precore protein derivatives, as well as p22 expressed without its signal peptide, were associated with autophagosomes. This result indicated that the association of p22 with autophagosomes did not require its signal peptide and supported the possibility that it was the cytosolic p22 that was associated with autophagosomes. Surprisingly, the core protein expressed by itself was not associated with autophagosomes and could not be detected in the immunoblot analysis. To confirm the immunoblot results, we conducted immunofluorescence microscopy. As shown in Fig. 4*C*, HBeAg was localized predominantly to the cytoplasm. Although there were not many autophagic puncta in $HBeAg^+$ cells as the precore protein by itself could not induce autophagy, the great majority of these autophagic puncta colocalized with HBeAg. No HBcAg could be detected in cells transfected with the precore protein-expressing plasmid. The p22 protein expressed without its signal peptide was detected primarily in the nucleus, although part of it was also detected in the cytoplasm. This result was consistent with what had previously been reported (9). Similar to the precore protein, p22 in the cytoplasm colocalized with the autophagic puncta. The same as the precore protein, no HBcAg could be detected in cells expressing p22. In contrast to precore proteins, HBcAg was detected primarily in the nucleus when the core protein was expressed by itself and, in agreement with the immunoblot results, no colocalization of HBcAg with autophagosomes was detected (Fig. 4*C*). Similarly, no HBeAg was detected in cells that expressed the core protein. The quantification of the colocalization efficiencies of precore, p22 and HBcAg with autophagosomes are shown in Fig. 4*D*. The results shown in Fig. 4*B*–*D* indicated that the core protein, when it was expressed by itself, could not be associated with autophagosomes. In contrast, the precore protein derivatives could be associated with autophagosomes in the absence of other HBV factors. The results shown in Fig. 4*C* also confirmed the specificity of our anti-HBeAg and anti-HBcAg antibodies.

HBV Core Protein but Not Precore Protein Is Associated with Phagophores. Phagophores are the precursor of autophagosomes. To determine whether the localization of precore and core proteins to autophagosomes was the result of their interaction with phagophores, we cotransfected Huh7 cells with the 1.3mer WT HBV genome and the expression plasmid of the mEmerald-ATG5 fusion protein. ATG5 is a marker of phagophores. At 48 h posttransfection, cells were lysed with a hypotonic buffer. A similar two-step purification protocol, which involved the isolation of cellular membranes by membrane flotation in a discontinuous sucrose gradient and the subsequent affinity purification using the anti-GFP antibody, was used to purify phagophores. Cells transfected with only the mEmerald-ATG5–expressing plasmid or the 1.3mer HBV genome were used as the controls. The purified phagophores were then subjected to immunoblot analysis. As shown in Fig. 5*A*, the core protein, but not the precore protein derivatives, was detected when phagophores purified from cells cotransfected with the mEmerald-ATG5–expressing plasmid and the 1.3mer HBV genomic DNA were analyzed. The association of the core protein with phagophores was specific and not due to contamination, as the core protein was not detected in cells transfected with only the HBV genomic DNA without the cotransfection of the mEmerald-ATG5–expressing plasmid. To further confirm the results, we also performed the immunofluorescence staining experiment. Cells were fixed and stained for the core particles using the anti-HBcAg antibody or for the precore protein using the anti-HBeAg antibody. As shown in Fig. 5*B*, HBV core particles in the cytoplasm colocalized with mEmerald-ATG5 puncta (i.e., phagophores), whether they were expressed from the WT HBV genome or the PC MT mutant. In contrast, there was little colocalization of HBeAg with phagophores, in agreement with the immunoblot results shown in Fig. 5*A*. The quantitative analysis of mEmerald-ATG5 puncta that were positive for core particles is shown in Fig. 5*C*.

The arginine-rich domain of the core protein contains multiple phosphorylation sites (36–38). To determine whether the association of the core protein with phagophores was regulated by its phosphorylation, we cotransfected Huh7 cells with the mEmerald-ATG5–expressing plasmid and the expression plasmid for the HBV core protein, the pCore-mutant 1 (CM1) core protein mutant or the pCore-mutant 2 (CM2) mutant. The expression plasmids for CM1 and CM2 had previously been generated in our laboratory (14, 36). CM1 contained the serine to alanine mutation in the three major phosphorylation sites located in the three SPRRR repeats in the arginine-rich domain of the core protein and resembled the hypophosphorylated core protein. In contrast, CM2 contained the serine to glutamic acid mutations in these three repeats and resembled the hyperphosphorylated core protein. As shown in *SI Appendix*, Fig. S2, the same as the WT core protein, both CM1 and CM2 core protein mutants colocalized with phagophores. This result indicated that the association of the core protein with phagophores was likely independent of its phosphorylation status.

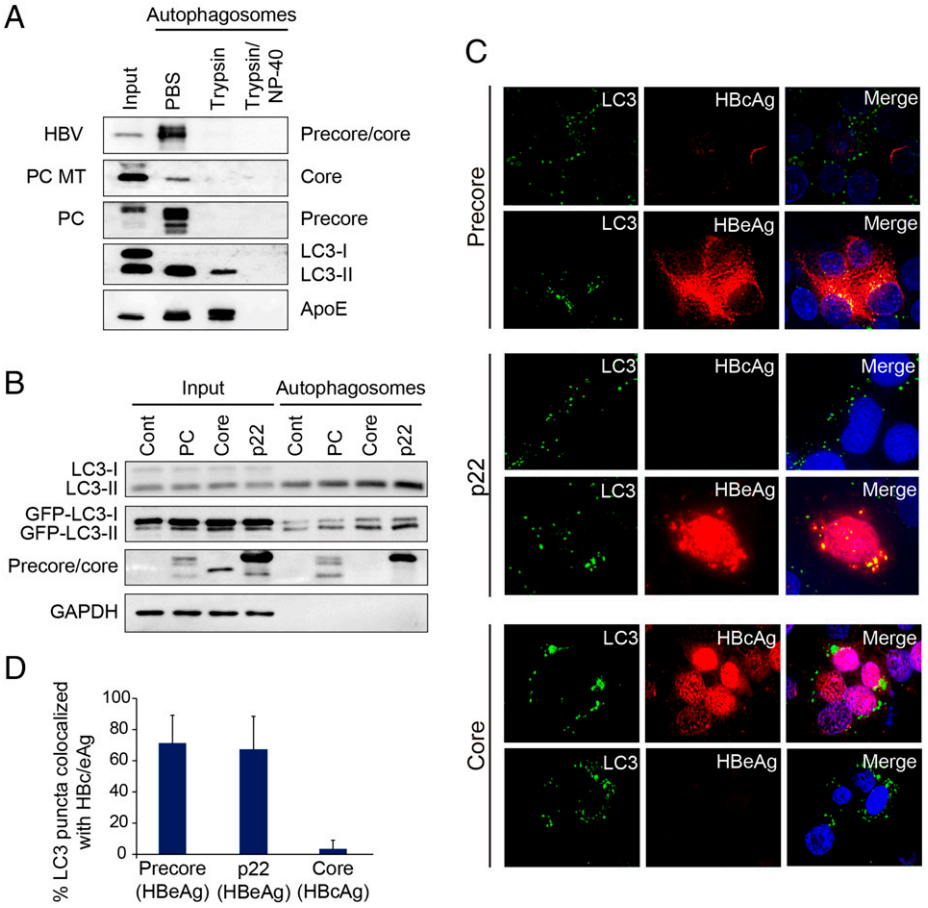

Fig. 4. Analysis of the association of precore and core proteins with autophagosomes. (*A*) The membrane protection assay was performed on autophagosomes that had been purified from Huh7-GFP-LC3 cells transfected with the HBV WT DNA, the PC MT DNA, or the precore protein (PC)-expressing plasmid. Autophagosomes were treated with PBS, trypsin or trypsin plus Nonidet P-40 (see *Materials and Methods* for details) followed by immunoblot analysis. Total cell lysates without treatment were used as the input control. (*B* and *C*) Huh7-GFP-LC3 cells were transfected with the expression plasmid of the PC, p22 without its signal peptide or the core protein. Immunoblot analysis was then conducted on total cell lysates or purified autophagosomes (*B*), and immunofluorescence microscopy was conducted to analyze the possible colocalizations between autophagosomes (green) and HBcAg or HBeAg (red) (*C*). Nuclei were stained with DAPI (blue). The cells were examined at 40x magnification. (*D*) Quantification of GFP-LC3 puncta (i.e., autophagosomes) that were positive for HBcAg or HBeAg. The results represented the average of >50 cells.

Core Particles Associated with Autophagic Membranes Are DNA Replication Competent. The observation that HBV core particles were associated with autophagosomes and phagophores in cells that were transfected with the HBV genomic DNA prompted us to examine whether these autophagic membrane-associated core particles contained replicating HBV DNA. Stable Huh7-GFP-LC3 cells that had been transfected with the HBV genomic DNA and Huh7 cells that were cotransfected with the mEmerald-ATG5–expressing plasmid and the HBV genomic DNA were used for the purification of autophagosomes and phagophores, respectively. Core particles associated with phagophores and autophagosomes, as well as those in the whole-cell lysates, which served as a positive control, were then analyzed by the endogenous polymerase assay and labeled with [α-^{32}P]-dCTP. As shown in Fig. 6*A*, two DNA bands, which represented the dsDNA and the single-stranded HBV DNA (ssDNA) (39), were detected when the whole-cell lysates were used for the analysis. When autophagosomes purified from Huh7-GFP-LC3 cells that had been transfected with the HBV genomic DNA were analyzed by the endogenous polymerase assay, two DNA bands were also detected, indicating that they contained DNA replication-competent core particles (Fig. 6*A*). The association of DNA replication-competent core particles with autophagosomes was not due to the nonspecific contamination of free core particles, as autophagosomes purified from Huh7 cells transfected with the HBV DNA failed to yield replicating DNA signals (Fig. 6*A*). When phagophores purified from Huh7 cells cotransfected with the mEmerald-ATG5–expressing plasmid and the HBV genomic DNA were analyzed, ^{32}P-labeled HBV DNA could also be detected, indicating that core particles associated with phagophores were also capable of replicating HBV DNA. Interestingly, in contrast to the whole-cell lysates and autophagosomes, which produced both dsDNA and ssDNA, phagophores produced mostly dsDNA, indicating that phagophores likely contained mostly core particles in the late stage of HBV DNA replication.

Previous studies indicated that the phosphorylation of the core protein was essential for pgRNA packaging and during this packaging process, the core protein was dephosphorylated, which was essential for HBV DNA replication (40–43). Thus, pgRNA- or DNA-containing core particles (i.e., nucleocapsids) contained only hypophosphorylated core protein (44). We had examined the phosphorylation status of the core protein associated with phagophores and autophagosomes using the NuPAGE gel, which allowed the separation of hyper- and hypophosphorylated core proteins (13). To reduce the complexity of protein bands on the gel, we used cells transfected with the HBV DNA that was incapable of expressing the precore protein for the studies (i.e., PC MT mutant). Phagophores and autophagosomes purified from cells were subjected to electrophoresis using the NuPAGE gel followed by immunoblot analysis. As shown in Fig. 6*B*, HBV core protein associated with

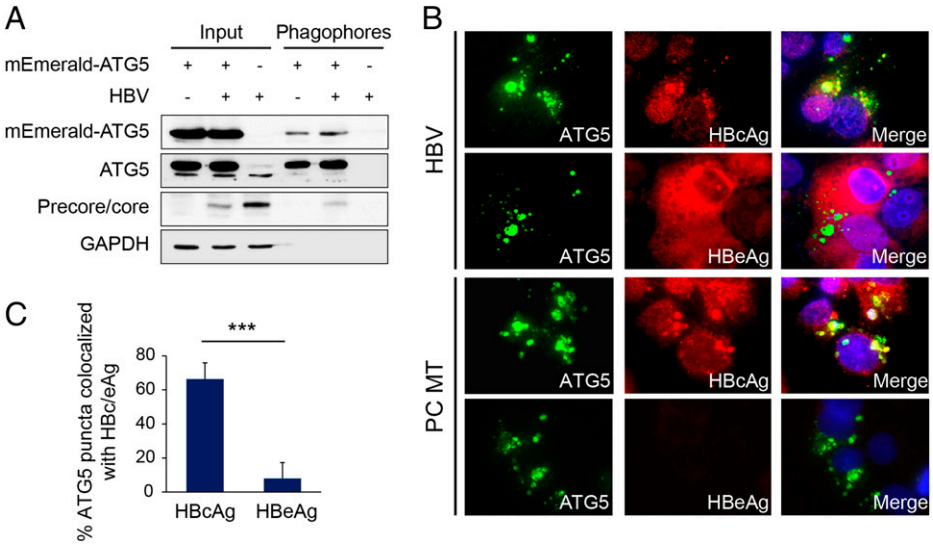

Fig. 5. Association analysis of HBV core and precore proteins with phagophores. (*A*) Immunoblot analysis of the whole-cell lysates (input) and phagophores that were purified from Huh7 cells that had been transfected with mEmerald-ATG5, the 1.3mer HBV WT genome, or both for 2 d. (*B*) Colocalization analysis of mEmerald-ATG5 (green) with HBcAg or HBeAg (red) in Huh7 cells that were cotransfected with the mEmerald-ATG5–expressing plasmid and the WT HBV genome or PC MT genome. DAPI was used to stain nuclei (blue). The cells were examined at 40x magnification. (*C*) Quantification of mEmerald-ATG5 puncta that were positive for HBcAg or HBeAg in *B*. The results represent the average of >50 cells.

autophagosomes was hypophosphorylated, although a low level of intermediately phosphorylated core protein could also be detected. In contrast, phagophores contained almost exclusively the hypophosphorylated core protein (Fig. 6*C*). These results indicate that most, if not all, of the core particles associated with these autophagic membranes were RNA- or DNA-containing particles.

Silencing of Rab11 Suppresses Viral Egress. MVBs play an important role in the egress of mature HBV particles. As autophagosomes can fuse with MVBs to form amphisomes, we investigated whether HBV-induced autophagosomes could also fuse with MVBs. As shown in Fig. 7*A*, CD63, a tetraspanin protein and a marker for MVBs (45), extensively colocalized with GFP-LC3 puncta in HBV^+ cells, indicating the formation of amphisomes. Rab11 is a small GTPase required for the formation of amphisomes (46–48). To determine whether it is also involved in the formation of HBV-induced amphisomes, we used small-interfering RNA (siRNA) to silence its expression. As shown in Fig. 7*B*, Rab11 silencing led to the reduction of autophagic puncta and their colocalization with CD63. Interestingly, it also increased the level of the core protein in cells (Fig. 7*C*). This increase was correlated with an increase of intracellular HBV DNA and a decrease of extracellular HBV DNA (Fig. 7*D*). The reduction of extracellular HBV DNA was also observed when virions and naked core particles were separately analyzed (*SI Appendix*, Fig. S3*A*). These results indicate the involvement of Rab11, a regulator of amphisomes, in HBV egress. In contrast to Rab11 silencing, the treatment of cells with bafilomycin A1, which inhibits autophagic degradation in autolysosomes as evidenced by the increase of p62 sequestosome and LC3 protein levels (*SI Appendix*, Fig. S3*B*), increased the precore/core protein level and both intracellular and extracellular HBV DNA levels (*SI Appendix*, Fig. S3*C*). This result indicates that the production and the release of progeny viral particles could also be negatively regulated by the late stage of autophagy.

Discussion

Previous studies indicated that autophagy played an important role in HBV DNA replication (28, 29). In this report, we demonstrate that HBV core particles containing replicating HBV DNA are associated with autophagosomes and phagophores (Figs. 1–3, 5, and 6). As the core protein associated with these autophagic membranes was mostly hypophosphorylated (Fig. 6*B* and *C*), which is a hallmark of mature HBV core

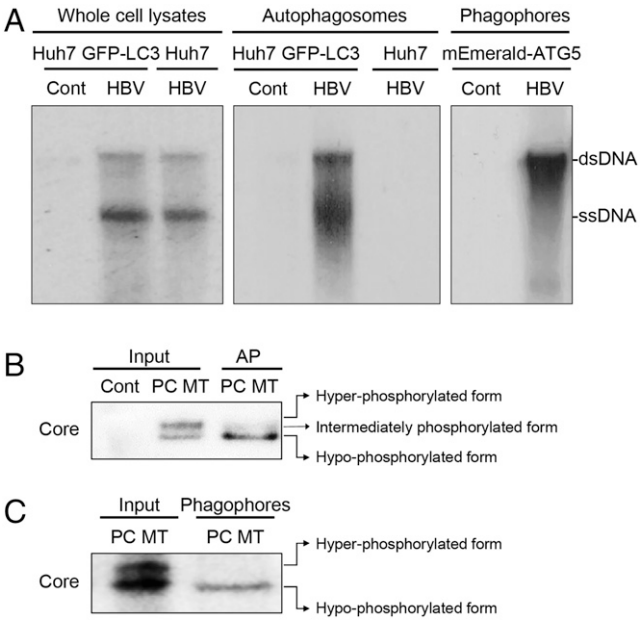

Fig. 6. DNA Replication-competent core particles are associated with both autophagosomes and phagophores. (*A*) The endogenous polymerase assay (EPA) was conducted using whole-cell lysates (*Left*), autophagosomes purified from Huh7-GFP-LC3 cells or Huh7 cells that had been transfected with pUC19 (Cont) or p1.3xHBV (*Center*), or phagohores purified from Huh7 cells that had been cotransfected with the mEmerald and pUC19 (Cont) or p1.3xHBV (*Right*). (*B*) Total cell lysates or autophagosomes purified from Huh7-GFP-LC3 cells transfected with pUC19 (Cont) or p1.3xHBV PC MT were subjected to electrophoresis in a NuPAGE gel followed by immunoblot to determine the phosphorylation status of the core protein. (*C*) Total cell lysates (input) and phagophores purified from Huh7 cells that had been cotransfected with the expression plasmids of mEmerald-ATG5 and p1.3xHBV PC MT were analyzed as in *B*. The locations of hyper-, intermediate-, and hypophosphorylated core protein bands were indicated.

particles (i.e., nucleocapsids), our results also indicate that most, if not all, of the core particles associated with autophagic membranes contained viral RNA or DNA. The phosphorylation of the core protein is required for the packaging of the pgRNA, which is associated with the dephosphorylation of the core protein. Our finding that the hyperphosphorylated core protein analog (i.e., CM2 mutant) could be localized to phagophores (*SI Appendix*, Fig. S2) is in support of the model that phagophores could serve as the platform for the packaging of the pgRNA, which likely took place immediately after the association of the hyperphosphorylated core protein with phagophores.

Previous reports indicated that the silencing of ATG5, ATG12, or ATG16 suppressed HBV DNA replication (29, 49). These previous reports further supported the importance of phagophores in the assembly of HBV nucleocapsids. The HBV core protein had been shown to bind to ATG12 (49). It is conceivable that this binding mediates the interaction between the core protein and phagophores and the subsequent encapsidation of the pgRNA. It should be noted that previous studies indicated that the silencing of ATG5 abolished HBV DNA replication but only slightly reduced the pgRNA packaging (28, 29). Thus, it is also possible that phagophores per se are not essential for the pgRNA packaging, and the core particles containing the pgRNA are merely piggybacked onto phagophores due to their interaction with ATG12. However, this association with phagophores is required for the subsequent HBV DNA replication. The observation that core particles associated with phagophores were in the more advanced stage of HBV DNA replication than those associated with autophagosomes is interesting (Fig. 6*A*). It is possible that phagophores may provide a niche to promote HBV DNA replication. Alternatively, it is also possible that the retention of core particles on phagophores delays their envelopment, prolonging their access to nucleotides for the completion of viral DNA replication. Note that, although our results provide compelling evidence to support a role of phagophores in pgRNA packaging and HBV DNA replication, additional studies will be required to confirm this observation.

Although core particles were found to be associated with phagophores and autophagosomes in cells harboring replicating HBV DNA, they were associated with phagophores but not autophagosomes when the core protein was expressed by itself. Our results indicate that the association of the core particles with autophagosomes was not dependent on the precore protein, surface proteins (Fig. 3), or viral DNA replication (*SI Appendix*, Fig. S1 *C* and *D*). How core particles became associated with autophagosomes and why this association required the presence of the HBV genome are unclear. One possible explanation is that, after their assembly on phagophores, core particles dissociate from phagophores and only those particles containing viral pgRNA or DNA are selectively reassociated with autophagosomes. This possibility is supported by our observation that a fraction of pgRNA or DNA-containing core particles was detected in the cytosolic fractions (Fig. 2*B* and *C*).

In contrast to the core protein, in cells that productively replicated HBV, precore protein derivatives were associated with autophagosomes but not with phagophores (Figs. 3 and 5 *A* and *B*). Previous studies indicated that the precore protein derivative p22 could be released back into the cytosol after the removal of its signal peptide by signal peptidase in the ER (8, 9). As precore protein derivatives were peripherally associated with autophagosomes (Fig. 4*A*), it is possible that the cytosolic

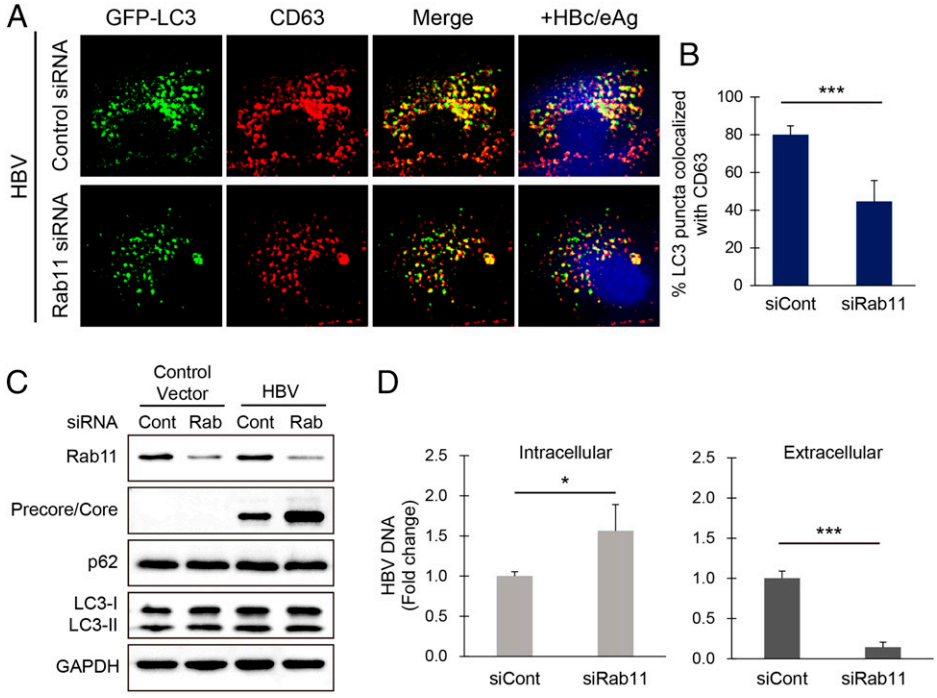

Fig. 7. Rab11 regulates egress of progeny HBV particles. (*A*) Huh7-GFP-LC3 cells treated with the control siRNA or the Rab11 siRNA were transfected with the HBV genomic DNA. The possible colocalization of autophagosomes (green) and CD63 (red) was analyzed by immunofluorescence microscopy. The merged images of GFP-LC3 puncta and CD63 were shown. HBeAg and HBcAg were also stained together (blue) using the antibodies directed against these two viral antigens. The cells were examined at 40x magnification. (*B*) Quantitative analysis of GFP-LC3 puncta that were positive for CD63. The results represented the average of >50 cells. (*C*) Immunoblot analysis of Huh7-GFP-LC3 cells that were treated with control siRNA or Rab11 siRNA and then transfected with pUC19 or the 1.3mer HBV genomic DNA. (*D*) qPCR of intracellular HBV DNA replicative intermediates in cells treated with either the control siRNA (siCont) or the Rab11 siRNA (siRab11). (*E*) qPCR analysis of extracellular viral particle-associated DNA. *$P < 0.05$; ***$P < 0.001$.

p22 was directly targeted to autophagosomes after its release from the ER. Our observation that p22 expressed without its signal peptide could be localized to autophagosomes supports this possibility (Fig. 4*B* and *C*). The biological function of the autophagosome-associated p22 remains to be determined. It is possible that the fusion between autophagosomes and MVBs will promote the interaction between p22 and Toll-like receptors (TLRs), which are inserted in endosomal membranes or plasma membranes, to disrupt the TLR signaling and host innate immune response, as previously reported (50).

MVBs play an important role in the release of mature HBV particles from cells (16–18). We found that the silencing of Rab11, which disrupted the fusion between autophagosomes and MVBs (Fig. 7*A* and *B*), reduced the extracellular HBV DNA level and in the meantime increased the intracellular HBV core protein and DNA levels (Fig. 7*C* and *D*). This finding agrees with a role of amphisomes in the egress of HBV virions, although the possibility that Rab11 silencing might have affected other properties of MVBs to result in the suppression of HBV egress cannot be ruled out. In contrast to Rab11 silencing, bafilomycin A1, which inhibits autophagic degradation in autolysosomes, increased HBV precore/core protein levels and intracellular and extracellular DNA levels (*SI Appendix*, Fig. S3 *B* and *C*). This increase of HBV protein and DNA levels might be due to the reduction of autophagic degradation of HBV particles and the increase of early autophagic membranes, which supported HBV replication.

In conclusion, our results indicate that autophagy plays multiple roles in the lifecycle of HBV: it provides the membranes for the assembly of HBV nucleocapsids, regulates the trafficking of HBV precore protein and core particles, and may also regulate the release of mature HBV virions.

Materials and Methods

Cell Cultures and HBV Infection. Huh7 cells and Huh7 cells that stably expressed GFP-LC3 (31) were maintained at 37 °C in Dulbecco's modified essential medium (DMEM) supplemented with 10% fetal bovine serum (FBS). Human hepatocytes (i.e., PXB cells) were prepared from uPA/SCID mice with humanized liver and used for the HBV infection experiment, as described previously (30). Briefly, PXB cells were infected with HBV (multiplicity of infection [MOI] = 100) obtained from HBV transgenic mouse serum in the presence of 4% polyethylene glycol (PEG). On day 1 postinfection, the culture medium was removed, and cells were washed thoroughly with phosphate-buffered saline (PBS) three times and incubated with the fresh medium containing 10% FBS and 2% dimethyl sulfoxide (DMSO). All animal work was conducted under the approval of the University of Southern California Institutional Animal Care and Use Committee in accordance with federal, state and local guidelines.

DNA Plasmids, siRNA, and DNA Transfection. The plasmid p1.3xHBV contains the overlength 1.3mer HBV genomic DNA in the pUC19 vector (51). p1.3xHBV PC^- (PC MT), and p1.3xHBV S^- (S MT) contained 1.3mer HBV genome with mutations that abolished the expression of the HBV precore protein and HBsAg, respectively. The S MT was constructed by mutating nucleotide 223 from T to A to generate a premature termination codon. This mutation did not affect the overlapping polymerase coding sequence. HBV protein expression plasmids, including pCMV-precore, pCMV-core, CM1, and CM2 had been described before (36). The plasmid pcDNA-p22 was constructed by deleting the signal peptide-coding sequence (amino acids 2 to 19) from pCMV-precore. The DNA plasmid mEmerald-ATG5-C-18 was purchased from Addgene (Addgene plasmid #54000). siRNA targeting human Rab11a (SASI_Hs01_00126206) and a negative control siRNA (SIC001) were purchased from Sigma-Aldrich. The DNA and siRNA transfections were performed using Lipofectamine 3000 (Invitrogen) and TransIT-X2 (Mirus) per the manufacturer's instructions.

Antibodies. The primary antibodies used in this study included the rabbit anti-LC3B antibody (Sigma), rabbit anti-GFP antibody (Cell Signaling), rabbit anti-p62 antibody (Cell Signaling), rabbit anti-LC3B antibody (Invitrogen), mouse anti-ApoE antibody (Santa Cruz), rabbit anti-ATG5 antibody (Cell Signaling), rabbit anti-HBsAg antibody (Novus Biologicals), mouse anti-CD63 antibody (Santa Cruz), and rabbit anti-Rab11a antibody (Invitrogen). Rabbit antibodies against HBcAg and HBeAg had been described previously (9). Briefly, the anti-HBcAg was produced by injecting rabbits using core particles expressed in *Escherichia coli*. The anti-HBeAg was prepared the same way with the exception that the core particles were denatured in SDS-mercaptoethanol prior to injection into rabbits. Secondary antibodies used for immunofluorescence were anti-rabbit and anti-mouse secondary antibodies conjugated with fluorescein isothiocyanate, rhodamine, or Alexa Fluor plus 405 (Invitrogen).

Immunoblot Analysis. Depending on the experiments, cells were lysed with M-PER mammalian protein extraction reagent (ThermoFisher) or with a hypotonic buffer. After a brief centrifugation to remove cell debris, cell lysates were subjected to SDS/PAGE or NuPAGE 12% Bis-Tris protein gel (Invitrogen) and transferred to a polyvinylidene difluoride (PVDF) membrane. The membrane was blocked with 5% skim milk for 45 min and incubated with the primary antibody overnight at 4 °C. After three washes with Tris-buffered saline (TBS) (10 mM Tris·HCl [pH 7.5], 150 mM NaCl) containing 1% Tween 20 (TBST), the membrane was incubated with horseradish peroxidase (HRP)-conjugated secondary antibody for 1 h. After washes with TBST, chemiluminescent substrates (Thermo Scientific) were added to the membrane, and the image was captured using the LAS-4000 imaging system (Fujifilm).

Immunofluorescence Staining and Microscopy. Cells were rinsed with PBS, fixed with cold acetone, permeabilized with PBS containing 0.1% saponin, 1% bovine serum albumin (BSA), and 0.05% sodium azide for 15 min, and then incubated with antibodies for immunofluorescence staining. Coverslips were mounted in ProLong Glass Antifade Mountant (Invitrogen) or Vector Shield (Vector) containing DAPI, which stained the nucleus. Images were acquired with a Keyence All-in-One fluorescence microscope. The colocalization efficiency, which measured the fraction of green fluorescent protein (GFP/mEmerald) pixels that were also positive for red pixels, was determined from randomly selected cells (>50) using the Keyence All-in-One software.

Membrane Flotation and Affinity Purification of Autophagic Membranes. The membrane flotation assay was performed as previously described (52). Briefly, cells seeded in two 10-cm plates were lysed with 500 μL hypotonic buffer (10 mM Tris·HCl [pH 7.5], 10 mM KCl, 5 mM $MgCl_2$), and passed through a 26-gauge needle at least 20 times. Next, nuclei and other cell debris were removed by centrifugation at 1,000 × *g* for 5 min at 4 °C. An aliquot of the supernatant was removed to serve as the input control, and the rest of the sample was mixed with 4 mL of 80% sucrose solution in the low-salt buffer (LSB) (50 mM Tris·HCl [pH 7.5], 25 mM KCl, and 5 mM $MgCl_2$) and overlaid with 4 mL of 55% sucrose solution, followed by the addition of 1.5 mL 10% sucrose solution in LSB. The sucrose gradient was centrifuged at 38,000 rpm in a Beckman SW40Ti rotor for 18 h at 4 °C. After centrifugation, 1-mL fractions were collected from the top of the gradient, and 20 μL of each fraction was subjected to immunoblot analysis. For the affinity purification, the membrane fraction was incubated with 50 μL anti-GFP monoclonal antibody-conjugated magnetic beads (MBL) at 4 °C overnight. The immune complex was then isolated with a magnetic separator for electron microscopy or immunoblot analysis.

Southern Blot and Primer-Extension Analysis. For Southern-blot analysis of HBV DNA, each sucrose fraction was treated with 10 units of DNase I (ThermoFisher) and micrococcal nuclease (New England Biolab) for 1 h at 37 °C to remove free DNA. The reaction was stopped by the addition of EDTA and proteinase K (300 μg/mL, ThermoFisher) and further incubated at 65 °C for 16 h as previously described (53). The HBV DNA packaged in core particles was then isolated by phenol-chloroform extraction and ethanol precipitation and analyzed by Southern blot using ^{32}P-labeled HBV DNA as the probe. The primer extension was performed as previously described (28). Briefly, to isolate the pgRNA packaged in core particles, cytosolic fractions 7 to 10, which were pooled, and fraction 3, which contained the membranes, were treated with DNase I and micrococcal nuclease for 1 h, as mentioned above. The sucrose in the samples was diluted

with 4 volumes of PBS, and core particles were pelleted by ultracentrifugation at 50,000 rpm in a Beckman SW55Ti rotor for 1 h at 4 °C. The core-associated pgRNA or total cellular RNA, which was used as the control, was extracted by TRIzol following the manufacturer's instructions (ThermoFisher). The oligonucleotide, 5′-GGT GAG CAA TGC TCA GGA GAC TCT AAG G-3′, which corresponds to nucleotides 2052 to 2025 of the HBV genome, was synthesized and used as the primer. To end-label the primer, 20 pmol of the oligonucleotide was mixed with 100 μCi of γ-[^{32}P]-ATP (Perkin-Elmer) and 10 units of T4 polynucleotide kinase for 1 h at 37 °C. The end-labeled primer was then purified using the QIAquick Nucleotide Removal Kit (Qiagen) and added to the RNA samples. The primer extension was carried out using SuperScript IV Reverse Transcriptase following the manufacturer's instructions (ThermoFisher). The reaction was stopped by phenol-chloroform extraction and ethanol precipitation. The samples were then analyzed on an 6% sequencing gel followed by autoradiography.

HBsAg and HBeAg ELISA. The incubation media of cells were harvested and analyzed for HBsAg and HBeAg using the ELISA kit following the manufacturer's instructions (International Immuno-Diagnostics). The medium was diluted 20-fold with PBS and 100 μL of diluted sample was used for the assay. The assays were conducted in triplicate.

Membrane Protection Assay. Affinity-purified autophagosomes were treated with 30 μL of 0.25% trypsin, 0.25% trypsin with 0.5% Nonidet P-40 (Nonidet P-40), or PBS at 37 °C for 1 h. PMSF (20 mM) was added after 1 h to stop the trypsin digestion reaction. The samples were then mixed with the protein sample buffer for SDS/PAGE.

Endogenous Polymerase Assay. Autophagosomes or phagophores that were affinity-purified using the anti-GFP–conjugated magnetic beads as described above were resuspended in the reaction mixture containing 50 mM Tris·HCl (pH = 7), 40 mM NH_4Cl, 20 mM $MgCl_2$, 0.1% Nonidet P-40 and 0.3% β-mercaptoethanol, 1 mM dNTP mixture, and α-^{32}P dCTP while they were still associated with the beads. The reaction mixture was incubated at 37 °C for 2 h. Next, 5 mM dCTP was added and continued the reaction for another hour at 37 °C. The reaction was stopped by adding 10% SDS, 50 mM EDTA, 10 mg/mL proteinase K and tRNA carrier, and further incubated at 65 °C for 2 h. The HBV DNA synthesized was then isolated by phenol-chloroform extraction and ethanol precipitation. The DNA pellet was rinsed with 70% ethanol and analyzed by agarose gel electrophoresis and autoradiography.

Intracellular and Extracellular HBV DNA Extraction. For cytoplasmic HBV DNA extraction, cells in 10-cm dishes were washed and lysed with lysis buffer (10 mM Tris·HCl [pH 7.5], 1 mM EDTA, 50 mM NaCl, and 0.1% Nonidet P-40). For extracellular HBV DNA extraction, the medium was centrifuged in a microfuge to remove cell debris followed by centrifugation at 50,000 rpm in a Beckman SW55Ti rotor for 1 h at 4 °C. The pellet, which contained both virions and naked core particles, was resuspended in PBS and treated with DNase I and micrococcal nuclease for 1 h at 37 °C to remove free DNA. Alternatively, 1 mL of the medium was first treated with DNase I and micrococcal nuclease for 1 h at 37 °C to remove free DNA, and then incubated with anti-HBsAg or anti-HBcAg overnight followed by the incubation with the Dynabeads Protein G (ThermoFisher) for 1 h. The beads were pelleted by centrifugation at 15,000 rpm for 1 min, washed with PBS four times and then treated with proteinase K. HBV DNA was isolated by phenol-chloroform extraction and ethanol precipitation. The DNA pellet was rinsed with 70% ethanol, dissolved in nuclease-free water and analyzed by Southern blot using the ^{32}P-labeled HBV DNA probe or by real-time PCR using the forward primer 5′-CCGTCTGTGCCTTCTCATCTG-3′, the reverse primer 5′-AGTCCTCTTATGTAAGACCTT-3′, and the TaqMan probe 5′-CCGTGTG CACTTCGCTTCACCTCTGC-3′, as described previously (33).

NuPAGE Gel Analysis of HBV Core Protein. Autophagic membranes were isolated by the two-step purification procedure. The immune complex associated with the magnetic beads was resuspended in NuPAGE LDS Sample Buffer (Invitrogen, NP0007) and heated at 95 °C for 5 min. The eluted immune complex was subjected to electrophoresis in NuPAGE 12% Bis-Tris protein gel (Invitrogen) using NuPAGE MES SDS Running Buffer (Invityrogen, NP0002) and transferred to a PVDF membrane using NuPAGE Transfer Buffer (Invitrogen, NP00061). The membrane was blocked with 5% skim milk for 45 min and incubated with the primary antibody overnight at 4 °C. After three washes with Tris-buffered saline (10 mM Tris·HCl [pH 7.5], 150 mM NaCl) containing 1% Tween 20 (TBST), the membrane was incubated with the HRP-conjugated secondary antibody for 1 h. After additional washes with TBST, chemiluminescent substrates (Pierce) were added to the membrane, and the image was captured using the LAS-4000 imaging system (Fujifilm).

Data Availability. All study data are included in the main text and *SI Appendix*.

ACKNOWLEDGMENTS. This work was supported by the NIH Grants AI148305, AI129540 and AI145813.

1. A. Schweitzer, J. Horn, R. T. Mikolajczyk, G. Krause, J. J. Ott, Estimations of worldwide prevalence of chronic hepatitis B virus infection: A systematic review of data published between 1965 and 2013. *Lancet* **386**, 1546–1555 (2015).
2. L. S. Y. Tang, E. Covert, E. Wilson, S. Kottilil, Chronic hepatitis B infection: A review. *JAMA* **319**, 1802–1813 (2018).
3. S. Tong, P. Revill, Overview of hepatitis B viral replication and genetic variability. *J. Hepatol.* **64** (1, suppl.), S4–S16 (2016).
4. J. H. Ou, O. Laub, W. J. Rutter, Hepatitis B virus gene function: The precore region targets the core antigen to cellular membranes and causes the secretion of the e antigen. *Proc. Natl. Acad. Sci. U.S.A.* **83**, 1578–1582 (1986).
5. F. Messageot, S. Salhi, P. Eon, J. M. Rossignol, Proteolytic processing of the hepatitis B virus e antigen precursor. Cleavage at two furin consensus sequences. *J. Biol. Chem.* **278**, 891–895 (2003).
6. M. A. DiMattia *et al.*, Antigenic switching of hepatitis B virus by alternative dimerization of the capsid protein. *Structure* **21**, 133–142 (2013).
7. K. Ito, K. H. Kim, A. S. Lok, S. Tong, Characterization of genotype-specific carboxyl-terminal cleavage sites of hepatitis B virus e antigen precursor and identification of furin as the candidate enzyme. *J. Virol.* **83**, 3507–3517 (2009).
8. P. D. Garcia, J. H. Ou, W. J. Rutter, P. Walter, Targeting of the hepatitis B virus precore protein to the endoplasmic reticulum membrane: After signal peptide cleavage translocation can be aborted and the product released into the cytoplasm. *J. Cell Biol.* **106**, 1093–1104 (1988).
9. J. H. Ou, C. T. Yeh, T. S. Yen, Transport of hepatitis B virus precore protein into the nucleus after cleavage of its signal peptide. *J. Virol.* **63**, 5238–5243 (1989).
10. M. L. Blondot, V. Bruss, M. Kann, Intracellular transport and egress of hepatitis B virus. *J. Hepatol.* **64** (1, suppl.), S49–S59 (2016).
11. J. Hu, C. Seeger, Hepadnavirus genome replication and persistence. *Cold Spring Harb. Perspect. Med.* **5**, a021386 (2015).
12. M. Nassal, Hepatitis B viruses: Reverse transcription a different way. *Virus Res.* **134**, 235–249 (2008).
13. Q. Zhao *et al.*, Hepatitis B virus core protein dephosphorylation occurs during pregenomic RNA encapsidation. *J. Virol.* **92**, e02139-17 (2018).
14. Y. T. Lan, J. Li, W. Liao, J. Ou, Roles of the three major phosphorylation sites of hepatitis B virus core protein in viral replication. *Virology* **259**, 342–348 (1999).
15. R. Prange, Host factors involved in hepatitis B virus maturation, assembly, and egress. *Med. Microbiol. Immunol. (Berl.)* **201**, 449–461 (2012).
16. S. F. Chou, M. L. Tsai, J. Y. Huang, Y. S. Chang, C. Shih, The dual role of an ESCRT-0 component HGS in HBV transcription and naked capsid secretion. *PLoS Pathog.* **11**, e1005123 (2015).
17. C. Lambert, T. Döring, R. Prange, Hepatitis B virus maturation is sensitive to functional inhibition of ESCRT-III, Vps4, and gamma 2-adaptin. *J. Virol.* **81**, 9050–9060 (2007).
18. T. Watanabe *et al.*, Involvement of host cellular multivesicular body functions in hepatitis B virus budding. *Proc. Natl. Acad. Sci. U.S.A.* **104**, 10205–10210 (2007).
19. C. He, D. J. Klionsky, Regulation mechanisms and signaling pathways of autophagy. *Annu. Rev. Genet.* **43**, 67–93 (2009).
20. D. Ganesan, Q. Cai, Understanding amphisomes. *Biochem. J.* **478**, 1959–1976 (2021).
21. Q. W. Teo, S. W. van Leur, S. Sanyal, Escaping the lion's den: Redirecting autophagy for unconventional release and spread of viruses. *FEBS J.* **288**, 3913–3927 (2021).
22. M. Ponpuak *et al.*, Secretory autophagy. *Curr. Opin. Cell Biol.* **35**, 106–116 (2015).
23. F. Reggiori, 1. Membrane origin for autophagy. *Curr. Top. Dev. Biol.* **74**, 1–30 (2006).
24. J. Geng, D. J. Klionsky, The Atg8 and Atg12 ubiquitin-like conjugation systems in macroautophagy. 'Protein modifications: Beyond the usual suspects' review series. *EMBO Rep.* **9**, 859–864 (2008).
25. Z. Xie, D. J. Klionsky, Autophagosome formation: Core machinery and adaptations. *Nat. Cell Biol.* **9**, 1102–1109 (2007).
26. D. C. Rubinsztein *et al.*, In search of an "autophagomometer". *Autophagy* **5**, 585–589 (2009).
27. D. Sir, J. H. Ou, Autophagy in viral replication and pathogenesis. *Mol. Cells* **29**, 1–7 (2010).
28. D. Sir *et al.*, The early autophagic pathway is activated by hepatitis B virus and required for viral DNA replication. *Proc. Natl. Acad. Sci. U.S.A.* **107**, 4383–4388 (2010).
29. Y. Tian, D. Sir, C. F. Kuo, D. K. Ann, J. H. Ou, Autophagy required for hepatitis B virus replication in transgenic mice. *J. Virol.* **85**, 13453–13456 (2011).
30. C. Yamasaki *et al.*, In vitro evaluation of cytochrome P450 and glucuronidation activities in hepatocytes isolated from liver-humanized mice. *Drug Metab. Pharmacokinet.* **25**, 539–550 (2010).
31. D. Sir *et al.*, Induction of incomplete autophagic response by hepatitis C virus via the unfolded protein response. *Hepatology* **48**, 1054–1061 (2008).
32. J. Li *et al.*, Subversion of cellular autophagy machinery by hepatitis B virus for viral envelopment. *J. Virol.* **85**, 6319–6333 (2011).
33. Y. Tian, C. F. Kuo, O. Akbari, J. H. Ou, Maternal-derived hepatitis B virus e antigen alters macrophage function in offspring to drive viral persistence after vertical transmission. *Immunity* **44**, 1204–1214 (2016).
34. D. R. Langley *et al.*, Inhibition of hepatitis B virus polymerase by entecavir. *J. Virol.* **81**, 3992–4001 (2007).
35. J. Y. Kim, J. J. Ou, Regulation of apolipoprotein E trafficking by hepatitis C virus-induced autophagy. *J. Virol.* **92**, e00211-18 (2018).

36. W. Liao, J. H. Ou, Phosphorylation and nuclear localization of the hepatitis B virus core protein: Significance of serine in the three repeated SPRRR motifs. *J. Virol.* **69**, 1025–1029 (1995).
37. M. J. Roossinck, A. Siddiqui, In vivo phosphorylation and protein analysis of hepatitis B virus core antigen. *J. Virol.* **61**, 955–961 (1987).
38. C. T. Yeh, J. H. Ou, Phosphorylation of hepatitis B virus precore and core proteins. *J. Virol.* **65**, 2327–2331 (1991).
39. S. Chaisomchit, D. L. Tyrrell, L. J. Chang, Development of replicative and nonreplicative hepatitis B virus vectors. *Gene Ther.* **4**, 1330–1340 (1997).
40. D. H. Perlman, E. A. Berg, P. B. O'connor, C. E. Costello, J. Hu, Reverse transcription-associated dephosphorylation of hepadnavirus nucleocapsids. *Proc. Natl. Acad. Sci. U.S.A.* **102**, 9020–9025 (2005).
41. J. Pugh, A. Zweidler, J. Summers, Characterization of the major duck hepatitis B virus core particle protein. *J. Virol.* **63**, 1371–1376 (1989).
42. P. Y. Su *et al.*, HBV maintains electrostatic homeostasis by modulating negative charges from phosphoserine and encapsidated nucleic acids. *Sci. Rep.* **6**, 38959 (2016).
43. Z. Hu *et al.*, Protein phosphatase 1 catalyzes HBV core protein dephosphorylation and is co-packaged with viral pregenomic RNA into nucleocapsids. *PLoS Pathog.* **16**, e1008669 (2020).
44. X. Ning *et al.*, Capsid phosphorylation state and hepadnavirus virion secretion. *J. Virol.* **91**, e00092-17 (2017).
45. Z. Andreu, M. Yáñez-Mó, Tetraspanins in extracellular vesicle formation and function. *Front. Immunol.* **5**, 442 (2014).
46. Z. Szatmári *et al.*, Rab11 facilitates cross-talk between autophagy and endosomal pathway through regulation of Hook localization. *Mol. Biol. Cell* **25**, 522–531 (2014).
47. C. M. Fader, D. Sánchez, M. Furlán, M. I. Colombo, Induction of autophagy promotes fusion of multivesicular bodies with autophagic vacuoles in k562 cells. *Traffic* **9**, 230–250 (2008).
48. Y. D. Chen *et al.*, Exophagy of annexin A2 via RAB11, RAB8A and RAB27A in IFN-γ-stimulated lung epithelial cells. *Sci. Rep.* **7**, 5676 (2017).
49. T. Döring, L. Zeyen, C. Bartusch, R. Prange, Hepatitis B virus subverts the autophagy elongation complex Atg5-12/16L1 and does not require Atg8/LC3 lipidation for viral maturation. *J. Virol.* **92**, e01513-17 (2018).
50. T. Lang *et al.*, The hepatitis B e antigen (HBeAg) targets and suppresses activation of the toll-like receptor signaling pathway. *J. Hepatol.* **55**, 762–769 (2011).
51. Z. Xu *et al.*, Enhancement of hepatitis B virus replication by its X protein in transgenic mice. *J. Virol.* **76**, 2579–2584 (2002).
52. J. Y. Kim, L. Wang, J. Lee, J. J. Ou, Hepatitis C virus induces the localization of lipid rafts to autophagosomes for its RNA replication. *J. Virol.* **91**, e00541-17 (2017).
53. Y. Zheng, J. Li, D. L. Johnson, J. H. Ou, Regulation of hepatitis B virus replication by the ras-mitogen-activated protein kinase signaling pathway. *J. Virol.* **77**, 7707–7712 (2003).